Journal of Petroleum Science and Engineering 144 (2016) 121–130

Contents lists available at ScienceDirect

Journal of Petroleum Science and Engineering

journal homepage: www.elsevier.com/locate/petrol

Non-hydrocarbon gas injection followed by steam–gas co-injection for heavy oil recovery enhancement from fractured carbonate reservoirs

A. Mohsenzadeh [a], M. Escrochi [a], M.V. Afraz [a], Gh. Karimi [a], Y. Al-Wahaibi [b,*], Sh. Ayatollahi [a]

[a] EOR Research Centre, Shiraz University, Shiraz, Iran
[b] Petroleum and Chemical Engineering Department, Sultan Qaboos University, Oman

ARTICLE INFO

Article history:
Received 23 April 2015
Received in revised form
11 March 2016
Accepted 12 March 2016
Available online 14 March 2016

Keywords:
Non-hydrocarbon gases
Gas injection
Steam-gas co-injection
Heavy oil
Fractured carbonate reservoirs

ABSTRACT

Considerable heavy oil is accumulated in naturally fractured carbonate reservoirs, with very low oil recovery efficiency through costly production techniques. In this experimental study, the effects of different non-hydrocarbon gases on the performance of gas injection process followed by steam–gas co-injection on heavy oil recovery from low permeable full sized carbonate cores were investigated at reservoir conditions in a long fractured laboratory model. Three different gases: pure CO_2, pure N_2, and their mixtures as synthetic flue gas were used to study the performance of gas injection process. Also, the tests were continued by steam–gas co-injection process that gas was injected with specific steam/gas ratio at steam saturation temperature condition. In the course of experiments, oil and water productions, pressure and temperature were monitored carefully.

It was found that during fracture depletion, the piston-like displacement by N_2 injection and oil foaming by CO_2 injection are the most important mechanisms affecting the oil recovery performance before gas breakthrough. The results showed that after gas breakthrough (GBT), the ultimate oil recovery based on residual oil at GBT for CO_2 injection was 58.4% (14.8% by gas injection and 43.6% by steam–gas co-injection), for flue gas injection was 73.8% (9.8% by gas injection and 64% by steam–gas co-injection) and for N_2 injection was 47% (13.5% by gas injection and 33.5% by steam–gas co-injection). The results of oil recovery and production rate indicated that the flue gas injection during gas injection and steam–gas co-injection processes was outperforming for heavy oil recovery enhancement from fractured reservoirs.

1. Introduction

In recent years, as global energy demand has increased and the production from conventional oil reservoirs declined, finding new oil resources has become an important challenge. Heavy oil is considered as one of the major resources of fossil fuel. Part of the large heavy oil reserves are accumulated in the naturally fractured carbonate reservoirs, where the fractures, in general, hold a small portion of the total oil: usually less than a few percent; and the remaining are accumulated within the matrixes (Haugen et al., 2010). In practice it has been demonstrated that plenty of oil remains in matrix blocks after primary production in the fractured reservoirs (Al-Shizawi et al., 1997; Saidi, 1996; Al-Hadhdarmi and Blunt, 2001).

Gas injection is highly recommended as a secondary production technique in naturally fractured carbonate reservoirs. It is stated that gas injection into the fractures activates gravity drainage, which leads to more oil recovery from the matrix blocks, preventing upward migration of the water level (Macaulay et al., 1995; Al-Hadhdarmi and Blunt, 2001; Nabipour et al., 2007). However, if this process is utilized in the case of heavy oil carbonate reservoirs; high oil viscosity and small, low permeable and predominantly oil-wet matrixes reduce oil production efficiency (Grattoni et al., 2001).

Oil production from matrix to the fractures is influenced by gravity forces, viscous forces, capillary forces, and mixing (diffusion or dispersion). During non-thermal immiscible gas injection process, owing highly conductive and interconnected fractures, viscose forces due to fluid flow through matrices are usually

Abbreviations: GOGD, Gas Oil Gravity Drainage; SAGD, Steam Assisted Gravity Drainage; IFT, Interfacial Tension; NCG, Non-Condensable Gas; GHG, Green House Gas; TC, Thermocouple; PT, Pressure Transducer; PLC, Programmable Logic Control; Soi, Initial Oil Saturation; Scw, Connate Water saturation; BPR, Back Pressure Regulator; GOC, Gas–Oil Contact; GBT, Gas Breakthrough; IOIP, Initial Oil in Place; IOIF, Initial Oil in Fracture; RO, Residual Oil; RF, Recovery Factor

* Corresponding author.
E-mail addresses: adel.mohsenzadeh@gmail.com (A. Mohsenzadeh), escrochi@gmail.com (M. Escrochi), vahidafraz@gmail.com (M.V. Afraz), ghkarimi@shirazu.ac.ir (Gh. Karimi), ymn@squ.edu.om (Y. Al-Wahaibi), shahab@shirazu.ac.ir (Sh. Ayatollahi).

http://dx.doi.org/10.1016/j.petrol.2016.03.003
0920-4105/

negligible compared to capillary forces (Verlaan and Boerrigter, 2006). Capillary forces adversely affect recovery of oil by gas injection because gas as a non-aqueous phase, can only displace the oil phase in the rock matrix from the fracture when it overcomes the capillary barrier. Therefore, in the immiscible gas injection process, gravity drainage and gas diffusion could be considered as the main governing mechanisms. Domination of each mechanism depends on different parameters such as size and permeability of matrix block, type of oil and injecting gas, pressure and temperature, size of fracture and rate of gas in the fracture. For example in low permeable and small matrix, since the capillary rise is high, gravity drainage is insufficient and gas diffusion is dominant (Chordia and Trivedi, 2010).

Considering the density difference between oil in the matrix and gas in the fracture as the only driving force for gas injection process; Maximum oil production rate due to gravitational force at one dimension vertical porous medium can be calculated from Darcy law. Assuming that no mixing occurs between phases, flow is incompressible and the oil viscosity and density remain constant (Chatzis and Ayalollahi, 1995; Kahrobaei et al., 2012; Al-Rabaani et al., 2008):

$$q_{grvity}=\frac{k_{rog}}{\mu_o}A\Delta\rho_{og}g \tag{1}$$

where k_{rog} is oil/gas relative permeability of the matrix, A is cross sectional area, μ_o is viscosity of oil and $\Delta\rho_{og}$ is density difference between oil and gas. Therefore, gas injection rate should be higher than maximum gravity drainage rate to make sure that the drained oil will be replaced by the injected gas.

1.1. Non-hydrocarbon gases injection in fractured reservoirs

CO_2 injection has several appealing technical and environmental advantages that attract many researchers, keeping it amongst the potential methods available for application in most hydrocarbon reservoirs. It is stated that miscibility condition for CO_2 and most crude oils, in practice starts at lower pressures than the other gases. On the other hand, for immiscible gas injection, CO_2 has higher density than other gases, which leads to smallest gas override problems. It is mentioned that carbon dioxide may be nearly as heavy as crude oil; however, this property reduces its gravity drainage driving force (Shawket, 2009; Mohsenzadeh et al., 2014)

Several studies have been presented in the literature on the concept of gas injection into fractured reservoirs. Darvish et al. (2006) used a fractured model to study the secondary and tertiary oil recovery by gas injection for live oil in a water-wet core at 300 bar and 130 °C, through modeling and experiments. The results revealed that diffusion is the main mechanism for matrix oil production and stated that gravity drainage has the least effects. Karimaie et al. (2008) performed several tests for secondary and tertiary injection of CO_2 and N_2 in a fractured carbonate model. They used synthetic live oil at reservoir conditions. The performed secondary experiments proved that most of the oil was recovered at considerably high rates during CO_2 injection, while N_2 flooding leads to only one fifth of CO_2 recovery at lower rates. They showed that secondary oil recovery was more effective than tertiary in CO_2 injection. Zhao et al. (2010) studied tertiary N_2 and CO_2 injection experimentally in a cubic model made of fractured carbonate rock. They showed that during oil production, the CO_2 efficiently changes the location of the oil-water interface, while N_2 maintains the pressure in the production zone due to its lower solubility both in oil and water phases. Hence, they expected an enhanced performance for the injection of N_2/CO_2 gas mixture in the field applications (Mohsenzadeh et al., 2014).

A brief review of the literature showed that the reported experimental studies in fractured models were mostly performed using light or synthetic oil in high permeable rock in range of 1–2 Darcy or sand pack models. With respect to the importance of heavy oil recovery from fractured reservoirs and the beneficial aspects of CO_2 injection into hydrocarbon reservoirs, further investigations of gas injection in a more consistent model is needed. It is critical to know that, during gas injection, the CO_2 concentration is the key parameter affecting the recovery factor. Therefore, Nitrogen, CO_2 and flue gases were selected here as the injecting fluids to establish gas injection to recover more heavy oil from laboratory fractured carbonate whole core model (Mohsenzadeh et al., 2014).

1.2. Steam-gas co-injection

Earlier experimental results and field applications for Gas Oil Gravity Drainage (GOGD) showed relatively low heavy oil recovery of around 10–20% at immiscible condition. The considerable amount of oil remains in the matrixes at the end of process when the depleted fractures are filled with the injecting gas and the reservoir is at the abandonment condition. This remaining oil is still a potential for suitable ongoing EOR applications which utilizes gravity drainage mechanism to increase heavy oil recovery. The application of thermal methods could be promising for the following steps of GOGD. Thermally assisted gas–oil gravity drainage (TA-GOGD) and steam assisted gravity drainage (SAGD) are employed for heavy oil recovery (Ayatollahi et al., 2005; Penney et al., 2007; Shahin et al., 2006; Mohsenzadeh et al., 2011). During most steam injection processes, the decline in chamber pressure due to cooling requires more steam injection compensation. Then, increases in steam–oil ratio, limit heavy oil recovery and there is no economic benefit to continue pure steam injection to make an effective thermal process. Several options were considered to overcome this phenomenon which the most promising one could be the injection of a non-condensable gas (NCG) such as CO_2, N_2 and CH_4 to replace the condensed steam, reduce heat loss to the overburden, and therefore, improve steam–oil ratio. The NCG maintains the chamber pressure and created a permanent gas phase across the top of the chamber therefore heat arrived to the producing well earlier (Bagci and Gumrah, 2004; Bagci et al., 2008). On the other hand, the steam-based thermal processes are energy intensive and cause high carbon dioxide (CO_2) emissions as a greenhouse gas (GHG). Regarding global forces to reduce greenhouse gas (GHG) emissions, there are potentials for the reduction of CO_2 emissions by capturing and disposal of CO_2 for pressure maintenance of these thermal operations. Previous studies pointed out various advantages for CO_2 addition to steam for heavy oil recovery. While pressure maintenance, depression of steam saturation temperature, reduction in steam–oil ratio, oil viscosity and IFT reduction and improving steam distillation process are recognized as the effects of CO_2 presence in steam injection (Mohsenzadeh et al., 2012; Tian et al., 2008; Bagci and Gumrah, 2004; Canbolat et al., 2004).

Nasr et al. (1987) examined the bitumen recovery from oil sands by continuous and cyclic injection of several steam–flue gas combinations. During the experiments, steam, steam–CO_2, steam–N_2 and steam–CO_2–N_2 mixtures were injected at 3.55 MPa and 100% steam quality into a high permeability oil sand bed. Experimental results indicated that the addition of flue gas to steam compared to steam-alone improves both rate and ultimate recovery of bitumen. Also they showed that the steam–CO_2 mixture was superior to either steam–N_2 or the steam–flue gas combinations. Bagci and Gumrah (2004) examined the special effects of simultaneous injection of CO_2 and CH_4 with steam on the recovery of 12.4 °API heavy oil from unconsolidated limestone. They found that Gas/steam ratio is an important factor among the studied variables in heavy oil recovery. While the depression of steam temperature was observed, lower residual oil saturations were obtained in gas-steam injection tests, compared to steam alone injection due to the presence of non-condensable gas. Tian et al. (2008), utilized laboratory physical sand packed model and a numerical simulation model to investigate the effects of CO_2 and surfactant addition to steam for heavy oil recovery. The effects of CO_2 dissolution in oil and water, variation of viscosity, oil volume and interfacial tension (IFT) during the recovery process were examined. They confirmed that viscosity reduction, oil foaming and IFT reduction play important roles enhancing heavy oil recovery. Their results showed that simultaneous CO_2 injection with steam improves heavy oil flow performance due to CO_2 dissolution in oil compared with steam injection only. At the same time, CO_2 decreases the temperature of steam front and effects on the expansion of steam chamber.

Al-Rabaani et al. (2008), showed the impact of matrix block heating rate on oil recovery rate by gravity drainage during Steam Assisted Gravity Drainage (SAGD). They performed analytic calculations and detailed numerical simulation for matrix-fracture network and both approaches confirmed that, the time taken to heat the matrix block could be similar or greater than the time taken for drainage of heated oil from matrix block. In these circumstances oil production is controlled by the rate at which the matrix block is heating up. They assumed that heat transfer within the matrix is dominated by conduction in the direction vertical to the fracture. Also, conduction in the matrix is negligible parallel to the fracture. Their results indicate that the oil recovery rate increases with increasing steam injection rate up to a critical steam injection rate. For higher steam rates, oil production rate remains constant. Also, they developed an analytical expression for estimating the optimum steam velocity which depends only on the matrix block size, water volumetric heat capacity and matrix block thermal conductivity as following:

$$U_{Cr} \approx \frac{2 l_x \lambda_m}{h l_z C_w} \tag{2}$$

where U_{Cr} is critical steam velocity (m/s), l_x is width or thickness of matrix block (m), l_z is height of matrix block (m), λ_m is thermal conductivity of the matrix (J/m s c), C_w is volumetric heat capacity of steam (J/m^3 c) and h is fracture aperture (m).

In this experimental work, heavy oil recovery from low permeable matrix in the long whole core fractured model was studied at reservoir condition. The immiscible gas injection process using non-hydrocarbon gases was applied in the first stage. In the second course of experiment, steam–gas co-injection was implemented to recover more heavy oil from the same gas-depleted model. The effects of gas type, based on different CO_2 compositions including pure CO_2, pure N_2 and their mixture as synthetic flue gas, on oil production and quality of processes were examined carefully (Mohsenzadeh et al., 2012).

2. Experimental

2.1. Experimental apparatus

Experimental setup and its schematic demonstration are shown in Fig. 1. A long high pressure core holder with 100 cm length and 10 cm inner diameter specially designed for the tests simulating fractured reservoir was the main part of the setup. For each test, six core samples with 15 cm length and 8.7 cm diameter were stacked vertically in the core holder. The annular space around the cores simulated vertical fracture, and the thin space between the six cores was considered as horizontal fractures where the capillary continuity is not completely maintained. The core holder was wrapped with a constant temperature thermal jacket maintain the core holder at constant temperature up to 350 °C. Accurate temperature and pressure transducers (TC and PT) were installed at specified places inside the core holder to monitor the temperature profile within the vertical fracture around the core samples. The temperature and pressure were also monitored on the injection line and on the production lines. Backpressure regulator was employed on the production line to keep the experiment at the constant pressure during production. A high temperature/high pressure steam generator was utilized to supply the injection fluids such as hot liquids and gases, saturated and superheated steam. The whole system was controlled using a Programmable Logic Control (PLC) unit, which monitored and

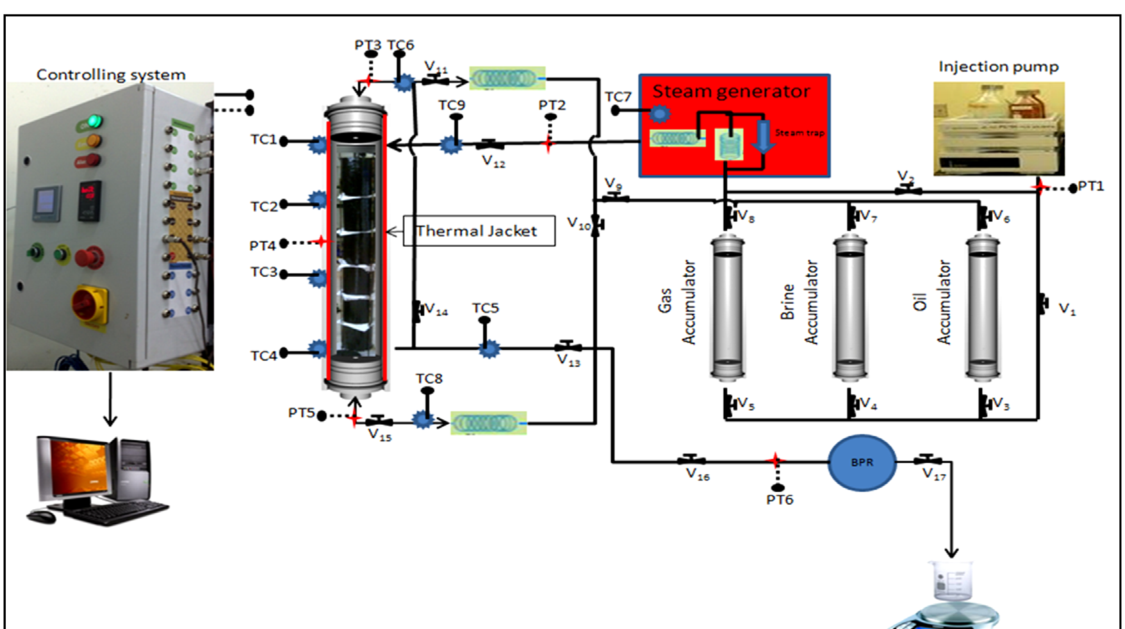

Fig. 1. Schematic illustration of the experimental setup.

Table 1
Dead crude oil and brine properties.

Crude Oil Bulk Properties	Property	Value	Property	Value	Viscosity of Crude Oil			
					Temperature (°C)			Viscosity (cP)
	Gravity	15.8 °API	Wax Content	2.5–3.5%	20			3860
					38			780
	Density @ 25 °C	959 kg/m^3	Asphaltene	~10 wt%	50			320
					82			74
					100			40
Crude Oil	**Comp.**	**Mole (%)**	**Comp.**	**Mole (%)**	**Comp.**	**Mole (%)**	**Mole Wt.(gr/gmol)**	**Sp. gr**
	N_2	0.001936	i-C_4	0.547153	$C_7{}^{+F}$	2.163434	120.77	0.9119
Composition properties	CO_2	0.022656	n-C_4	1.56041	$C_7{}^{+G}$	8.414434	171.09	0.9328
	C_1	0.336199	i-C_5	1.505817	$C_7{}^{+H}$	16.45902	249.20	0.9480
	C_2	0.196848	n-C_5	2.266857	$C_7{}^{+I}$	22.38638	363.69	0.9608
	C_3	0.823227	n-C_6	5.5287	$C_7{}^{+J}$	37.78694	681.10	0.9800
Formation Brine Properties	**Property**		**Value**		**Ion**		**Composition (mg/L)**	
	Salinity as NaCl		123000 PPM		**Calcium**		6600	
	TDS		125.512		**Magnesium**		1882	
	Color		Slightly yellow		**Sodium**		41638	
	pH		5.5		**Chloride**		80940	
	Specific Gravity		1.088		**Sulfate**		280	
	Viscosity		1.05 cP		**Bicarbonate**		171	

C7$^{+F,G,H,I \text{ and } J}$ are different groups of C7^{+}.

recorded the important parameters of the system such as temperature and pressure as well as maintaining the tests at the pre-specified experimental conditions (Mohsenzadeh et al., 2012, 2014)

To saturate the core plugs with brine and oil, special Hassler type core holder for whole core size were utilized which could handle 8.7 cm diameter and up to 30 cm length core plugs. The core holder was equipped with thermal jacket and confining pressure system to operate at high temperature and pressure up to 350 °C and 6000 psi. In addition, for brine, oil and gas injection, three high pressure piston-cylinder accumulators were used. Injection rate was controlled with HPLC pump by injection of distilled water to other side of accumulator at constant flow rate at desire pressure.

2.2. Materials and methods

Heavy crude oil from one of the South Iranian carbonate reservoirs with 15.8 °API and viscosity of 3860 cp at 25 °C was used during the experiments. Properties of the utilized heavy crude oil and actual formation brine are presented in Table 1.

Core samples were selected from a relatively homogeneous carbonate outcrop of reservoir formation. The core samples with 15 cm length and 8.7 cm diameter had the porosity range of 14–20%, and the low permeability range between 3.5 and 9.5 mD. Each fresh and dry core sample was vacuumed and saturated with actual formation brine from the field (Table 1). Porosity of each core was calculated based on brine density and weight difference between dry core and saturated core with formation brine. The saturated core plug was transferred to the Hassler-type core holder. Brine was injected for liquid (absolute) permeability measurement using Darcy law. Then, heavy oil was injected to the brine saturated core until the core reached the initial oil saturation (Soi) and connate water saturation (Scw) conditions. Finally, the saturated core samples were aged for 30 days in crude oil at 80 °C to restore reservoir wettability condition. The previous studies on wettability alteration of the same rock have shown that maximum oil wetness condition is gained stabilized wetting properties after approximately 30 days of aging. Aging beyond this period does not have a major impact (Roosta et al., 2009; Seiedi et al., 2010). The wettability alteration was confirmed through contact angle measurements which are shown in Fig. 2. Comparison between contact angle of water droplet on the surface of fresh core sample and aged core sample shows that the wettability changed from strongly water wet towards neutral wet condition.

Three gas mixtures with different CO_2 volume ratio were chosen to be injected into vertically mounted long core holder at reservoir condition to monitor heavy oil production at immiscible state. The utilized gases consisted of pure CO_2, mixture of 15% CO_2 and 85% N_2 as a synthetic flue gas and pure N_2. The synthetic flue gas composition was selected based on the reported compositions in the literature for exhausted gas of natural gas power plants

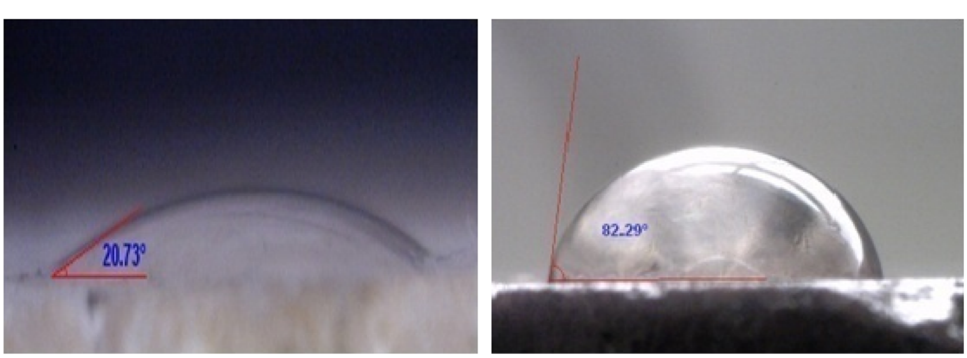

Fig. 2. Contact angle measurement by water droplet, fresh core=20.73° (left side, strongly water wet), aged core=82.29° (right side, Neutral wet).

Table 2
Experimental conditions.

Test no.		1	2	3
Injected gas		**CO_2**	Flue gas **(15% CO_2 +85% N_2)**	**N_2**
Calculated MMP at 80 °C Using CMG WINPROB 2007.11		**4300 Psi**	**13250 Psi**	**13200 Psi**
Initial Conditions				
Matrix properties	**Porosity of each plug From top to bottom**	**20**	**17.7**	**17.5**
		19.7	**17.5**	**17.2**
		19.3	**17.1**	**16.7**
		19	**16.8**	**15.8**
		18.2	**16.5**	**14.9**
		18	**16.1**	**14**
	Ave. Porosity	**19%**	**17%**	**16%**
	Permeability of each plug From top to bottom	**9.5**	**7.5**	**7.3**
		8.8	**7.2**	**6.8**
		8.1	**6.7**	**6.0**
		7.5	**6.3**	**5.2**
		7.2	**5.8**	**4.3**
		7.1	**5.6**	**3.5**
	Ave. Permeability	**8 md**	**6.5 md**	**5.5 md**
	Total Length	**6 × 15 cm**	**6 × 15 cm**	**6 × 15 cm**
	Core Diameter	**8.7 cm**	**8.7 cm**	**8.7 cm**
Matrix Saturations	**S_{wi}**	**20.5**	**21.2**	**23.3**
	S_{oi}	**79.5**	**78.8**	**76.7**
Matrix liquid Volumes	**Water**	**208 cm^3**	**193 cm^3**	**199 cm^3**
	Oil	**807 cm^3**	**717 cm^3**	**658 cm^3**
Fracture oil Volume		**2218 cm^3**	**2196 cm^3**	**2260 cm^3**

(Nasr et al., 1987; Zhang et al., 2004; Yee and Stroich, 2004).

2.3. Experimental procedure

The experimental procedure included four main steps:

- As illustrated in Fig. 1, the set of six 15 cm oil-saturated and aged core samples with almost the same porosity and permeability values were stacked with tissue in between for capillary continuity. The 90 cm matrix block transferred to the long core holder and the same crude oil was injected to fill and pressurize the system up to 750 psi. Temperature of core holder was increased to 80 °C and the amount of oil produced due to the thermal expansion through the back pressure regulator (BPR) was measured. These experimental conditions were selected to duplicate the same conditions of target heavy oil fractured reservoir and were kept constant during the experiments using thermal jacket. Details of core properties and experimental conditions in each test are reported in Table 2.
- A water table, simulating a bottom aquifer, was formed by water injection from the bottom of the core holder at constant pressure. This water level was kept constant at the level of production line during the experiments.
- Maximum gravity drainage rate of 0.037 cm^3/min was roughly calculated by Eq. (1) at atmospheric pressure and 80 °C using absolute permeability values instead of relative permeability. Therefore, gas injection from the top of core holder was preceded in two different stages at the rates higher than maximum oil drainage rate: in the first stage, gas was injected at the rate of 5 cm^3/min to produce oil from the fractures and forcing Gas–Oil Contact (GOC) downward until gas breakthrough. In the second stage, since the oil production after gas breakthrough is mainly from the matrixes at the extremely lower rates, the gas injection rate was subsequently reduced to 1 cm^3/min for pushing the produced oil into the production line (Mohsenzadeh et al., 2014; Darvish et al., 2006).
- When Gas Oil Ratio (GOR) reached to 100%, saturated steam at the rate of 0.5 cm^3/min based on cold water with gas at the rate of 1 cm^3/min were co-injected through steam generator. The amount of condensed water and produced oil were measured and monitored versus time until no more oil production and achieving 100% water cut (Mohsenzadeh et al., 2012). It should be noted that steam injection rate was chosen based on calculation of critical steam injection rate by Eq. (2) as following:

$$q_{cr}=\frac{U_{cr}}{A} \tag{3}$$

$$A = \frac{\pi}{4}\left(D_i^2-D_c^2\right) \tag{4}$$

where q_{cr} is critical steam injection flowrate, U_{cr} is critical steam velocity from Eq. (2), A is the cross sectional area open to steam flow, D_i and D_c are inner diameter of core holder and core diameter, respectively. For this experimental system, critical steam injection flowrate was about 20 cm^3/min at 750 psi and steam saturation temperature. Also, by simulating the steam generator in AspenHysys V7.2 simulator and utilizing SRK equation of state, 20 cm^3/min saturated steam at 750 psi was equal to 0.5 cm^3/min based on cold water at ambient condition.

3. Results and discussion

Oil production from fractured reservoirs with a natural or secondary gas cap drive could be continued until the gas-invaded zone reaches production wells, known as gas breakthrough, which results in considerable increase in GOR. This process corresponds to the depletion of the oil zone and critical production decline in the fractured reservoirs known as economic recovery efficiency. In the following tests, gas was injected at initially at high rate to recover the oil from the fracture and reach to gas breakthrough, then the gas injection rate was lowered for oil production from the matrixes, which was also performed by previous studies to mimic the oil recovery from fractured reservoirs with gas cap drive mechanism (Darvish et al., 2006). The oil production results and the performances of these two steps are compared in this section. Experimental conditions and the results are summarized in Tables 2 and 3.

3.1. Oil production before gas breakthrough

During the first step of gas injection, the amount, rate and foaming factor of the produced oil were monitored carefully before gas breakthrough. The results are presented in Table 3, along with Figs. 4 and 5. The produced oil before gas breakthrough was found to be foamy, as shown in Fig. 3. The gas bubbles were then released and settled produced oil was collected and measured volumetrically. Fig. 4 shows the foaming factor, which is the ratio of produced foamy oil volume to the remaining oil volume in the graduated cylinder after settling. This parameter also corresponds to the foaming effects of the injected gas into the oil zone. It can be seen that the foaming factor increased with time, when the maximum value was achieved just before gas breakthrough. Among different types of gases, the highest foaming factor or foam quality was observed during the CO_2 injection test, which was considerably less for the flue gas and N_2 tests respectively.

The observations showed that when the CO_2 was part of the injected gas, the produced oil was foamy. It was the indication of a stable foam zone formation at the bottom of the gas invaded zone

Table 3
Experimental results.

Test no.	1	2	3
Production before Gas Breakthrough			
Oil production (cm^3)	2066.1	2155.6	2281.8
Average production rate before GBT	7.28 (Scm^3/min)	8.47 (Scm^3/min)	5.61 (Scm^3/min)
RF at GBT (%IOIP)	68.3	74.0	78.2
RF at GBT (% IOIF)	92.9	98.1	100.1 (Fractured oil + 3.4% Matrix oil)
Average oil Foaming factor before GBT	3.65 (cm^3/Scm^3)	1.46 (cm^3/Scm^3)	1.33(cm^3/ Scm^3)
RO at GBT	959 cm^3	757 cm^3	636 cm^3
Production after Gas Breakthrough			
Production (cm^3) Oil	141.8	74.5	85.4
Water	16.8	10	26
Average oil production rate	0.0067 (cm^3/min)	0.0035 (cm^3/min)	0.0040 (cm^3/min)
RF (%RO at GBT)	14.8	9.8	13.5
Ultimate RF (%IOIP)	72.9	76.5	81.1
Steam–Gas co injection			
Average Steam–Gas Temperature (°C)	155	170	175
Delay time to oil production (hr)	2	70	65
Total injected steam (cm^3 of water)	13255.5	12197.5	25326
Produced oil (cm^3)	309	486.7	286.3
Total produced water (cm^3)	10691	8988.8	21432.8
Steam/oil ratio	43	25	88
Average oil production rate (cm^3/min)	0.020	0.060	0.01
RF (% RO after Gas Injection)	37.8	71.1	52
Ultimate RF (% RO at GBT)	47	73.8	58.4

which leads to early breakthrough of the gas, while a portion of the oil was still remained unattainable in the fracture part. But in case of no foamy oil (N_2 injection), complete fracture depletion as well as partial oil recovery from the matrixes at gas breakthrough was occurred, while the oil recovery at gas breakthrough based on the initial oil in fracture was only 98.1% and 92.9% for flue gas and CO_2 respectively. Besides, the highest oil production rate before gas breakthrough was observed during flue gas injection, while the lowest was achieved in N_2 injection.

Previous study on foamy oil viscosity measurement by Al-Shmakhy and Maini (2012) showed that below the bubble point, once the solution gas starts to release, the viscosity of a stable foamy-oil with low gas volume fractions (Foam quality) was very close to live-oil viscosity. While at higher foam quality, foamy-oil viscosity increased and became much higher than the original live-oil viscosity and finally it approaches to dead-oil viscosity. In addition, measurements by prior studies have shown non-Newtonian behavior of foamy-oil at high gas volume fractions (Al-Shmakhy and Maini, 2012). Therefore, the viscosity of foamy-oil should be considered as an effecting mechanism of oil production from fracture. Results of recovery factor and production rate could be evidence that the mutual effects of oil foaming and piston-like displacement of the oil, within the fracture, are controlling the oil recovery. The results demonstrated that the optimum oil foaming causes maximum oil production rate, while efficient piston type displacement leads to maximum oil recovery in fracture depletion; therefore the optimal contribution of both mechanisms should be considered before gas breakthrough (Zhao et al., 2010).

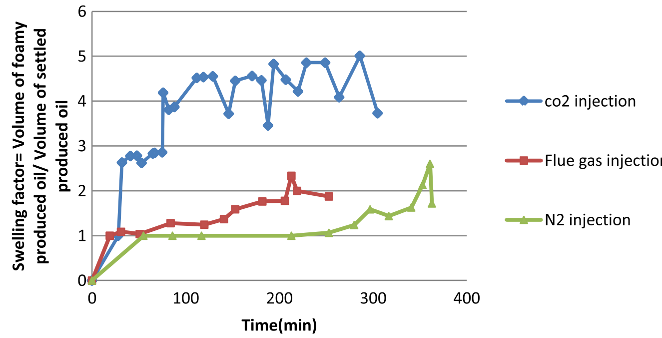

Fig. 4. Oil foaming factor during the gas injection before GBT.

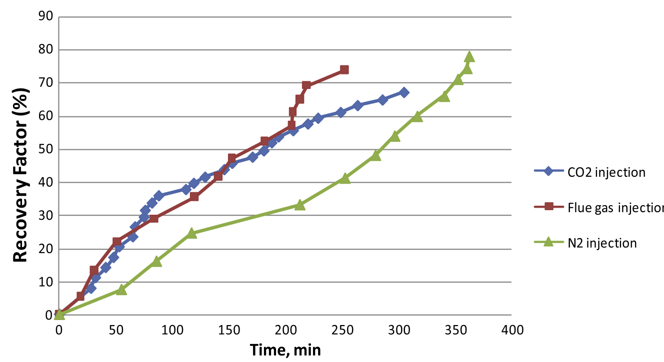

Fig. 5. Oil recovery factor by gas injection before GBT based on IOIP.

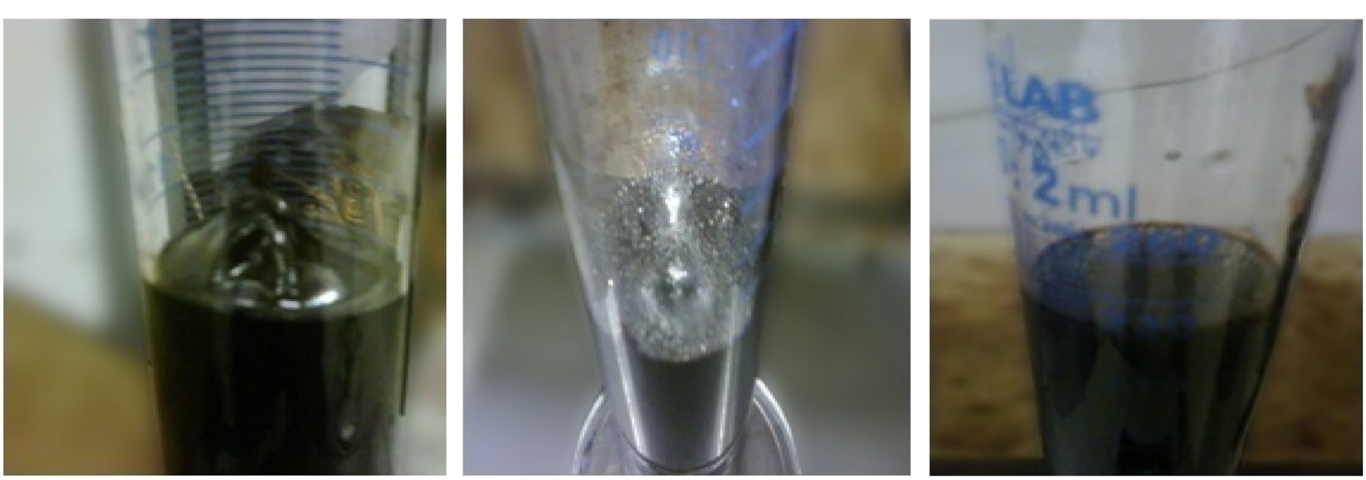

Fig. 3. Foamy produced oil before GBT during (a) CO_2 injection, (b) Flue gas injection and (c) N_2 injection.

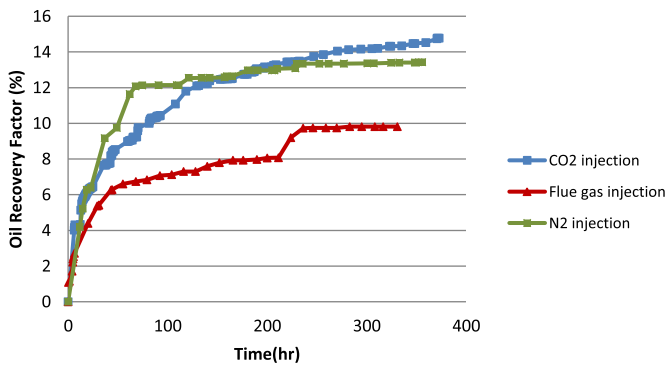

Fig. 6. Oil Recovery factor by gas injection based on residual oil at GBT.

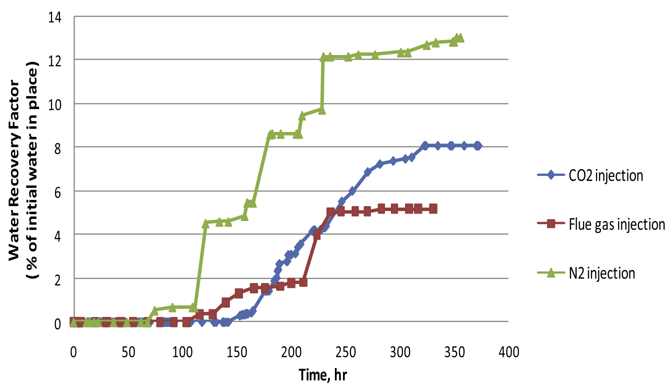

Fig. 7. Water production recovery factor based on initial water in matrix.

3.2. Oil and water production after gas breakthrough

Economical oil production is usually limited by the undesired fluids production, which dramatically increases after gas/water breakthrough at the reservoir depletion conditions. However, the field experiences have shown that the produced oil before gas breakthrough is mainly from the fractures, which is not a considerable portion of the oil in place in most of the fractured reservoirs (Haugen et al., 2010). While, the major fraction of the oil remains in the matrixes is produced mainly after gas breakthrough. In this study, the oil production after gas breakthrough was also monitored carefully and the ultimate performance of gas injection (using different type of gases) was determined. The results of oil and water productions are presented in Table 3, Figs. 6 and 7. The results indicated that the CO_2 injection was outperforming to the other gases. The oil recovery was 14.8%, 9.8% and 13.5% with respect to the remaining oil at gas breakthrough for CO_2, flue gas and N_2 injection, respectively.

On the other hand, the average oil production rate after gas breakthrough as the main parameter governs the profitability of the project was measured for each test and the results are reported in Table 3. As it is shown, the highest production rate was noticed for CO_2 injection test of 0.0067 cm^3/min. However, for flue gas and N_2 tests, the oil production rate was almost the same around 0.0035 and 0.0040 cm^3/min, respectively. Also, Comparison between values of actual oil production rate in the experiments and analytical maximum drainage rate by Eq. (1) which is 0.037 cm^3/min, shows the actual rates are less than analytical rate. It should be noted that in Eq. (2), absolute permeability is used, but in the experiments, oil, water, gas, steam were all present in the pore space, and the relative permeability should be employed instead of the absolute value. In addition, the difference between actual and analytical oil production rates can be attributed to capillarity; compressibility of gas phase and density increase at high pressure; gas dissolution and mixing between oil and gas in the fracture (which was observed during production before GBT) which leads to a lower density difference and thus a lower drainage rate (Ameri et al., 2013).

When pure CO_2 is injected, it diffuses into the oil-saturated matrixes resulting in oil expansion and viscosity reduction, which causes more oil recovery at higher production rate from the matrixes (Zhao et al., 2010; Shawket, 2009). Besides, the density difference as the driving force for gravity drainage, in the case of N_2 injection, is the greatest factor that increases oil recovery. However, for flue gas injection, CO_2 molecules tend to diffuse into the liquid phase, while the bulk of N_2 molecules accumulate in the pathway reducing the displacement potential of the oil film to flow in the pores and throats leading to more oil trapping in the matrixes (Nabipour et al., 2007). Therefore, from the both results of recovery factors and oil production rates, it can be deduced that the gravity drainage because of density difference between oil and gas, and gas diffusion are the two main mechanisms of oil recovery from the matrixes after gas breakthrough (Darvish et al., 2006; Karimaie et al., 2007; Zhao et al., 2010).

The results of water production during gas injection after gas breakthrough are illustrated in Fig. 7. The mechanism by which the water was produced from the cores is mainly water/gas gravity drainage (Darvish et al., 2006). Water production along with oil recovery during all three tests, demonstrated that fluid displacement took place within the matrixes and the displaced oil was produced from the matrixes. In addition, as it is shown in Fig. 7, the delay times for water production increased with increasing of CO_2 content in the injected gases. It proved that in the early stage of oil production after gas breakthrough, the gas diffusion and oil foaming were the dominant mechanisms during CO_2 and flue gas injections, which prevent water flow until critical saturation of oil is attained in the matrixes. While during N_2 injection, the density difference between gas phase and liquid phases caused both oil and water flow in porous media and production by gravity drainage.

As shown in Table 3, the ultimate oil recovery for N_2 injection was more than the other two tests. Evidently, more foaming aptitude of the crude–gas mixture causes oil trapping in the fracture part, which results in less ultimate recovery from the laboratory model; however, in the field scale the ratio of the oil in the matrixes to the fracture is more, therefore CO_2 injection seems to be more efficient for the field cases. However, it should be highlighted that the heavy oil recovery from carbonate matrixes was as low as 10–15% in these tests. This confirms that in such reservoirs, immiscible gas injection should be assisted by other compatible mechanisms, such as miscible gas injection or steam injection methods (Mohsenzadeh et al., 2014)

3.3. Secondary steam–gas co-injection

In this stage steam was enriched with the same gas from previous step and injected into the model. Gas at the rate of 1 cm^3/min and steam at the rate of 0.5 cm^3/min (based on cold water) were injected simultaneously through the steam generator to the top of core holder. The heavy oil and condensed water were collected from the bottom of the model at the constant pressure condition of 750 psi through the back pressure regulator and the volumetric amounts were measured carefully during the tests. The summary of experimental conditions and results are reported in Tables 2 and 3. Besides, the incremental results of oil recovery during the all three tests are shown in Figs. 8 and 9.

3.3.1. Heavy oil recovery enhancement

Fig. 8 shows the results of oil recovery factor during steam–gas co-injection process. It is based on the remaining oil after earlier

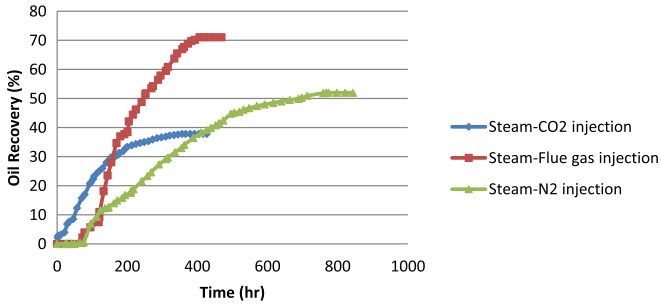

Fig. 8. Oil recovery factor by steam–gas injection based on residual oil after gas injection.

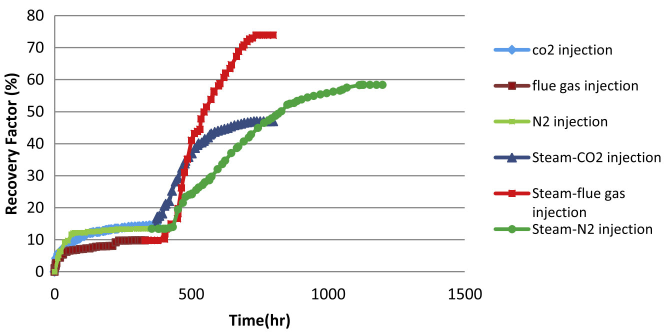

Fig. 9. Oil recovery factor by gas injection and steam–gas co-injection based on residual oil at GBT.

gas injection process. The first considerable point is the delay time between the steam–gas injection startup and the first drop of oil production. This time period for steam–CO_2 injection was about 2 h, while for steam–flue gas injection and steam–N_2 injection, it was around 70 h. It seems the early oil production during steam–CO_2 injection was as a result of production of foamy remaining oil in the fracture which was stable and non-producible by earlier gas injection. On the other hand, the results of delay time for steam–flue gas and steam–N_2 injection show that the oil production in the thermal methods require a thermally steady state condition in the whole matrixes for the oil displacement. Asadizadeh et al. (2014) conducted almost the same tests and studied the secondary and tertiary thermally induced gas–oil gravity drainage. They also reported this delay time between initiation of steam injection and starting time of oil production. They showed that in the early hours of steam injection, viscosity reduction was the dominant mechanism and after that the following oil production was because of the gravity drainage mechanism.

The results of ultimate oil recovery factor, average production rate and total injected steam during the steam–gas co-injection process are reported in Table 3. The highest oil recovery factor based on oil in place after the earlier gas injection stage was by steam–flue gas injection of about 71.1%. While this amount by steam–N_2 injection was 52% and the lowest recovery factor was achieved in steam–CO_2 injection process. Adversely, the average oil production rate during the steam–flue gas injection test was the highest around 0.06 cm^3/min compared to the rate of oil production during steam–CO_2 injection test of about 0.02 cm^3/min and the lowest one for steam–N_2 injection at 0.01 cm^3/min. The previous studies also reported similar results that co-injection of CO_2 with steam could accelerate and improve oil recovery rate (Mohsenzadeh et al., 2012; Zhong et al., 2013; Monte-Mor et al., 2013).

3.3.2. *Steam saturation temperature and steam–oil ratio*

A double stage steam generator was designed to produce saturated mixture of steam and gas for this experimental setup. Distilled water and gas are passed the first stage and heated up to saturated temperature. At the end of first stage, a steam trap separates and recycles the hot water. Then, the produced vapor is passed the second stage and heated once more to guarantee that the outlet mixture from the steam generator is at saturated condition. During the tests, temperature of steam–gas mixture right before injection point to the core holder was measured and monitored. The average injection temperature of steam–gas mixture for all three tests is shown in Table 3. The results indicated that, compared to the steam saturation temperature, the presence of CO_2 in the mixture results in more reduction of the steam–gas saturation temperature. For example, the saturation temperature of the pure steam from the steam table at 750 psi is about 245 °C, while this value for steam–CO_2 mixture was about 155 °C, for the case of steam–flue gas mixture was 170 °C and for steam–N_2 mixture was around 175 °C. The previous studies have shown that, the exact amount of reduction in saturation temperature for steam–gas mixture depends on the injection pressure, gas type and steam–gas ratio (Mohsenzadeh et al., 2012; Monte-Mor et al., 2013; Feng et al., 2012).

Furthermore, the total amount of injected steam which is an important parameter which indicates energy consumption during thermal method was calculated. Results of total injected steam based on injected cold water showed that the presence of CO_2 in the injecting gas mixture considerably reduces the steam–oil ratio. Total volume of injected steam during the steam–CO_2 injection test was 13,255.5 cm^3 for 309 cm^3 of oil recovery (steam–oil ratio of 43) while for the steam–flue gas injection process, it was 12,197.5 cm^3 for 486.7 cm^3 oil recovery (steam–oil ratio of 25).The results also showed that, this value for steam–N_2 injection test was 25326 cm^3 steam for 286.3 cm^3 of oil recovery (steam–oil ratio of 88). This shows the economical value of the Steam Flue gas co-injection compared to the other two methods used in this study.

3.3.3. *Steam accumulation in chamber*

Fig. 10 shows the incremental amounts of remaining steam in the system during the period of steam–gas injection. Since heavy oil, gas and condensed water were produced through production line during steam–gas co-injection, it indicated that there was no accumulated condensed water remaining in the fracture. Therefore, the amount of steam in the heated chamber was calculated based on differences between volume of injected water and volume of produced water at the same time. As it is shown, the amount of steam in the chamber was increased linearly during steam–CO_2 and steam–flue gas injection tests. However, for the steam–N_2 injection test it shows increasing trend until it achieved the maximum value, then it remained approximately steady up to the end of the test. At the beginning of steam–gas injection to the gas invaded fractures, the steam saturation in the fractures are increased up to the thermodynamic equilibrium values for all the tests. On the other hand, the dissolution of CO_2 and flue gas in the

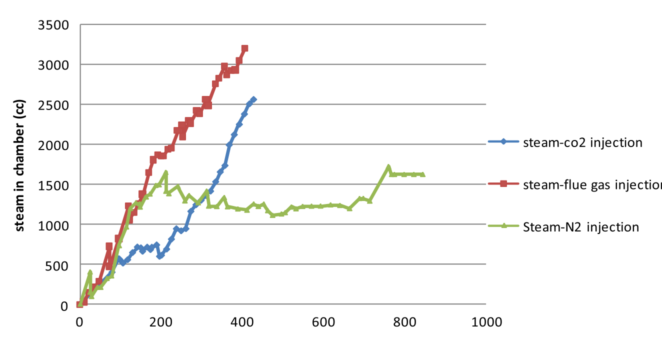

Fig. 10. Steam in chamber during steam–gas co-injection.

produced heavy oil caused reduction of gas composition in the steam–gas mixture within the fractures which resulted in more steam accumulation in the steam chamber. But, for steam–N_2 injection test, the slight gas dissolution in the produced oil caused the constant composition of steam and gas inside the chamber after achieving the equilibrium saturation condition.

In summary, the results of this study showed that the steam–flue gas injection for heavy oil recovery from fractured model was outperforming compared to steam–CO_2 injection and steam–N_2 injection tests. However, choosing the most efficient one is not very simple. Since, steam–N_2 injection caused high ultimate oil recovery, while the average oil production rate, steam–oil ratio, the amount of energy (steam) consumption and the CO_2 sequestration for the steam–CO_2 injection test were more favorable. Therefore, economical factors, environmental aspects of CO_2 sequestration, oil price, energy consumption, oil demands, production rate and ultimate recovery should be considered all together carefully to choose the most efficient method. Besides, the optimum composition of CO_2/N_2 in the gas mixture for steam–gas co-injection should be obtained by economical study of flue gas purification process and more oil recovery tests involving different CO_2/N_2 ratios with field application objectives (Mohsenzadeh et al., 2012).

4. Conclusions

Non-hydrocarbon gas injection process and secondary steam–gas co-injection tests were investigated for heavy oil recovery enhancement from fractured carbonate experimental model at specified reservoir conditions. The full size low permeable and oil-wet core samples were used in the long core holder and the effects of three different gases such as pure CO_2, pure N_2 and mixture of 15% CO_2 and 85% N_2 as synthetic flue gas were utilized.

- It was found that oil recovery before gas breakthrough was mostly from the fracture part. Results showed that the piston wise displacement by N_2 injection leads to maximum fracture oil recovery, while the presence of CO_2 in the injected gas forms stable foamy oil within the fracture, leading to more oil trapping in the fracture and decrease of heavy oil recovery before gas breakthrough. Furthermore, the highest oil production rate with reasonable fracture oil recovery efficiency was achieved due to the combination of foaming effects and piston wise displacement for the case of flue gas injection.
- The results of gas injection after gas breakthrough showed that, the oil recovery factors from the matrix for CO_2 injection (due to gas diffusion effects) and for N_2 injection (as a result of highest oil-gas density difference) were the same of about 14% of OOIP. However, during the flue gas injection the combination of these two mechanisms resulted in lower recovery factor about 9%.
- Secondary steam–gas co-injection experiments showed that steam–flue gas injection for heavy oil recovery from fractured model was outperforming compared to steam–CO_2 injection and steam–N_2 injection tests.
- Choosing the most efficient gas is complicated. Since, steam–N_2 injection showed high ultimate oil recovery, while the average oil production rate, steam–oil ratio, the amount of energy (steam) consumption and the CO_2 sequestration for the steam–CO_2 injection test were more favorable. Therefore, economical factors, environmental aspects of CO_2 sequestration, oil price, energy consumption, oil demands, production rate and ultimate recovery should be considered all together carefully to choose the most efficient method. Besides, the optimum composition of CO_2/N_2 in the gas mixture for steam–gas co-injection should be obtained.

SI metric conversion factors

psi $\times$ 6.894 757 E+00 = kPa
°F (°F − 32)/1.8 = °C
°API 141.5/(131.5 + °API) = g/cm^3
ft $\times$ 3.048*E − 01 = m
cp $\times$ 1.0*E − 03 = Pa s
bar $\times$ 1.0*E + 05 = Pa
in. $\times$ 2.54*E + 00 = cm
*Conversion factor is exact.

References

Al-Hadhdarmi, H., Blunt, M., 2001. Thermally induced wettability alteration to improve oil recovery in fractured reservoirs. SPE Reserv. Eval. Eng. 4 (3), 179–186. http://dx.doi.org/10.1218/71866-PA (SPE-71866-PA).

Al-Shizawi, A., Denby, P.G., Marsden, G., 1997. Heat-Front Monitoring in the Qarn Alam Thermal GOGD Pilot. Paper SPE 37781-MS presented at the Middle East Oil Show and Conference, Bahrain 15-18 March. http://dx.doi.org/10.1218/37781-MS.

Al-Shmakhy, B., Maini, B.B., 2012. Foamy-Oil-Viscosity Measurement. J. Can. Pet. Technol. 51 (1), 60–65. http://dx.doi.org/10.2118/136665-PA.

Al-Rabaani, A.S., Blunt, M.J., Muggeridge, A.H., 2008. Calculation of a critical steam injection rate for thermally-assisted gas-oil gravity drainage. In: Proceedings of Paper SPE 113351 presented at the 2008 SPE/DOE Improved Oil Recovery Symposium held in Tulsa, Oklahoma, USA, 19–23 April. http://dx.doi.org/10.1218/113351.

Ameri, A., Farajzadeh, R., Suicmez, V.S., Verlaan, M., Bruining, J., 2013. Effect of non-equilibrium gas injection on the performance of (immiscible and miscible) gas − oil gravity drainage in naturally fractured reservoirs. J. Energy Fuels 27, 6055–6067. http://dx.doi.org/10.1021/ef401372d.

Asadizadeh, S., Mohsenzadeh, A., Escrochi, M., Ayatollahi, Sh., Roayaei, E., 2014. Secondary and tertiary thermally induced gas-oil gravity drainage from oil- wet fractured rocks: experiments under reservoir conditions. J. Energy Sources Part A: Recovery Util. Environ. Eff. 36 (16), 1818–1826. http://dx.doi.org/10.1080/15567036.2011.563263.

Ayatollahi, Sh., Boukadi, F., Wadhahi, M., Bemani, A., 2005. Investigation of thermal gas–oil gravity drainage (GOGD) in fractured carbonate reservoirs. In: Proceedings of Paper SPE 93585-MS presented at the 14th Middle East Oil and Gas Show and Conference, Kingdom of Bahrain, 12–15 March. http://dx.doi.org/10.1218/93585-MS.

Bagci, A.S., Olushola, S., Mackay, E., 2008, Performance analysis of SAGD wind-down process with CO_2 injection. In: Proceedings of Paper SPE 113234-MS presented at SPE Symposium on Improved Oil Recovery, 20–23 April, Tulsa, Oklahoma. http://dx.doi.org/10.1218/113234-MS.

Bagci, A.S., Gumrah, F., 2004. Effects of CO_2 and CH_4 addition to steam on recovery of West Kozluca heavy oil. In: Proceedings of Paper SPE 86953-MS Presented at the SPE International Thermal Operations and Heavy Oil Symposium, 16–18 March, Bakersfield, California. http://dx.doi.org/10.1218/113234-MS.

Canbolat, S., Akin, S., Kovescek, A.R., 2004. Noncondensable gas steam assisted gravity drainage status and scope for EOR development in Oman. J. Pet. Sci. Technol. 45, 83–96.

Chatzis, L., Ayalollahi, Sh., 1995. Investigation of the gaigi process in stratified porous media for the recovery of waterflood residual oil. In: Proceedings of Paper SPE 95-139 Presented at Technical Meeting/Petroleum Conference of The South Saskatchewan Section, October 16–18, Regina. http://dx.doi.org/10.2118/95-139.

Chordia, M., Trivedi, J.J., 2010. Diffusion in naturally fractured reservoirs – a review. In: Proceedings of Paper SPE 134589 Presented at the SPE Asia Pacific Oil & Gas Conference and Exhibition held in Brisbane, Queensland, Australia, 18–20 October 2010. http://dx.doi.org/10.2118/134589-MS.

Darvish, G.R., Lindeberg, E., Holt, T., Utne, S.A., Kleppe, J., 2006. Reservoir-conditions laboratory experiments of CO_2 injection into fractured cores. In: Proceedings of Paper SPE 99650 Presented at the SPE Europec/EAGE Annual Conference and Exhibition, Vienna, Austria, 12–15 June. http://dx.doi.org/10.1218/99650-MS.

Feng, Q., Guo, L., Zhang, X., Gao, S., Shi, S., Wu, S., 2012. Study of thermal recovery Method of Steam and Flue gas combined with Gel Injection. In: Proceedings of SPE 157928 Presented at the SPE heaby oil conference Canada held in Calgary, Alberta, Canada, 12–14 June. http://dx.doi.org/10.1218/157928-MS.

Grattoni, C.A., Jing, X.D., Dawe, R.A., 2001. Dimensionless groups for three-phase gravity drainage flow in porous media. J. Pet. Sci. Eng. 29 (1), 53–65.

Haugen, A., Fernø, M.A., Bull, Ø., Graue, A., 2010. Wettability impacts on oil displacement in large fractured carbonate blocks. J. Energy Fuels 24 (5), 3020–3027. http://dx.doi.org/10.1021/ef1000453.

Kahrobaei, S., Farajzadeh, R., Suicmez, V.S., Bruining, J., 2012. Gravity-enhanced transfer between fracture and matrix in solvent-based enhanced oil recovery. In: Proceedings of Paper SPE 154171 Presented at the Eighteenth SPE Improved Oil Recovery Symposium held in Tulsa, Oklahoma, 14–18 April. http://dx.doi.org/10.1218/154171-MS.

Karimaie, H., Darvish, G.R., Lindeberg, E., Torsæter, O., 2007. Experimental investigation of secondary and tertiary gas injection in fractured carbonate rock. In: Proceedings of Paper SPE 107187 Presented at the SPE Europec/EAGE Annual Conference, London, United Kingdom, 11–14 June. http://dx.doi.org/10.1218/1071887-MS.

Macaulay, R.C., Krafft, J.M., Hartemink, M., Escovedo, B., 1995. Design of a steam pilot in a fractured carbonate reservoir – Qarn Alam Field, Oman. In: Proceedings of Paper SPE 30300 Presented at the International Heavy Oil Symposium, Calgary, Alberta, Canada, 19–21 June. http://dx.doi.org/10.1218/30300-MS.

Mohsenzadeh, A., Nabipour, M., Asadizadeh, S., Nekouie, M., Ameri, A., Ayatollahi, Sh, 2011. Experimental investigation of different steam injection scenario during SAGD process. Spec. Top. Rev. Prous Media: Int. J. 2 (4), 281–293. http://dx.doi.org/10.1615/STRPM.v2.i4.30.

Mohsenzadeh, A., Escrochi, M., Afraz, M.V., Ayatollahi, Sh., Karimi, Gh., Al-wahaibi, Y., 2014. The effects of CO_2 concentration in flue gas injection for heavy oil recovery from fractured reservoirs during GOGD process. In: Proceedings of Paper SPE 169707-MS Presented at the SPE EOR Conference at Oil and Gas West Asia held in Muscat, Oman, 31 March–2 April. http://dx.doi.org/10.1218/169707-MS.

Mohsenzadeh, A., Escrochi, M., Afraz, M.V., Al-wahaibi, Y., Ayatollahi, Sh. 2012. Experimental investigation of heavy oil recovery from fractured reservoirs by secondary steam–gas assisted gravity drainage. In: Proceedings of Paper SPE 157202-MS-P Presented at the SPE Heavy Oil Conference Canada held in Calgary, Alberta, Canada, 12–14 June. http://dx.doi.org/10.1218/157202-MS-P.

Monte-Mor, L.S., Laboissière, P., Trevisan, O.V., 2013. Laboratory study on steam and flue gas co-injection for heavy oil recovery. In: Proceedings of Paper SPE 165523 Presented at the SPE Heavy Oil Conference Canada held in Calgary, Alberta, Canada, 11–13 June. http://dx.doi.org/10.1218/165523-MS.

Nabipour, M., Escrochi, M., Ayatollahi, Sh., Boukadi, F., Wadhahi, M., Maamari, R., Bemani, A., 2007. Laboratory investigation of thermally-assisted gas–oil gravity drainage for secondary and tertiary oil recovery in fractured models. J. Pet. Sci. Eng. 55 (1–2), 74–82. http://dx.doi.org/10.1016/j.petrol.2006.04.013.

Nasr, T.N., Prowse, D.R., Frauenfeld, T., 1987. The use of flue gas with steam in bitumen recovery from oil sands. J. Can. Pet. Technol. 26 (3), 62–69. http://dx.doi.org/10.2118/87-03-06.

Penney, R., Baqi Al Lawati, S., Hinai, R., et al., 2007. First full field steam injection in a fractured carbonate at Qarn Alam, Oman. In: Proceedings of Paper SPE 105406-MS Presented at the SPE Middle East Oil and Gas Show and Conference, Kingdom of Bahrain, 11–14 March. http://dx.doi.org/10.2118/105406-MS.

Roosta, A., Escrochi, M., Varzandeh, F., Khatibi, J., Ayatollahi, Sh., 2009. Investigating the mechanism of thermally induced wettability alteration. In: Proceedings of Paper SPE 120354 Presented at the SPE Middle East Oil and Gas Show and Conference, Bahrain, 15–18 March. http://dx.doi.org/10.1218/120354-MS.

Saidi, A.M., 1996. Twenty years of gas injection history into well-fractured Haft Kel Field (Iran). In: Proceedings of Paper SPE 35309 Presented at the International Petroleum Conference and Exhibition of Mexico, Villahermosa, Mexico, 5–7 March. http://dx.doi.org/10.1218/35309-MS.

Seiedi, O., Rahbar, M., Nabipour, M., Emadi, M.A., Ghatee, M.H., Ayatollahi, Sh., 2010. Atomic force microscopy (AFM) investigation on the surfactant wettability alteration mechanism of aged mica mineral surfaces. J. Energy Fuels 25 (1), 183–188. http://dx.doi.org/10.1021/ef100699t.

Shahin, Jr. G.T., Moosa, R., Kharusi, B., Chilek, G., 2006. The physics of steam injection in fractured carbonate reservoirs: engineering development options that minimize risk. In: Proceedings of Paper SPE 102681-MS Presented at the SPE Annual Technical Conference and Exhibition. San Antonio, Texas, September 24–27. http://dx.doi.org/10.1218/102681-MS.

Shawket, G., 2009. Global laboratory experience of CO_2-EOR flooding. In: Proceedings of Paper SPE 125581 Presented at the SPE/EAGE Reservoir Characterization and Simulation Conference, Abu Dhabi, UAE, 19–21 October. http://dx.doi.org/10.1218/125581-MS.

Tian, S., He, S., Qu, L., 2008. Investigating the effect of steam, CO_2, and surfactant on the recovery of heavy oil reservoirs. In: Proceedings of Paper SPE-PS2008-365 Presented at the SPE International Thermal Operations and Heavy Oil Symposium held in Calgary, Alberta, Canada, 20–23 October. http://dx.doi.org/10.1218/PS2008-365.

Verlaan, M., Boerrigter, P., 2006. Miscible gas/oil gravity drainage. In: Proceedings of Paper SPE 103990 Presented at the First International Oil Conference and Exhibition in Mexico held in Cancun, Mexico, 31 August–2 September. http://dx.doi.org/10.1218/103990-MS.

Yee, C.T., Stroich, A., 2004. Flue gas injection into a mature SAGD steam chamber at the dover project (formerly UTF). J. Can. Pet. Technol. 43 (1), 54–61. http://dx.doi.org/10.2118/04-01-06.

Zhang, Y.P., Sayegh, S.G., Huang, S., Dong, M., 2004. Laboratory investigation of enhanced light-oil recovery by CO_2/flue gas huff-n-puff process. J. Can. Pet. Technol. 45 (2), 24–32. http://dx.doi.org/10.2118/06-02-01.

Zhao, R.B., Ke, W.Q., Wu, Y.H., Zhao, H.Y., Yue, X.A., 2010. Enhanced heavy oil recovery from fractured vuggy carbonated reservoir of tahe oilfield with N_2/CO_2 gas mixture. In: Proceedings of Paper SPE 132247 Presented at the International Oil and Gas Conference. Beijing, China, 8–10 June. http://dx.doi.org/10.2118/132247-MS.

Zhong, L., Dong, Z., Hou, J., Li, Y., Sun, Y., Zhao, L., Lu, W., Qin, F., 2013. Investigation on principles of enhanced offshore heavy oil recovery by coinjection of steam with flue gas. In: Proceedings of Paper SPE 165231 Presented at the SPE Enhanced Oil Recovery Conference held in Kuala Lumpur, Malaysia, 2–4 July. http://dx.doi.org/10.2118/165231-MS.

Adel Mohsenzadeh, holds B.Sc. and M.Sc. degree in chemical and petroleum engineering from Shiraz University, Shiraz, Iran. Currently he is Ph.D. Student of petroleum engineering at Sultan Qaboos University (SQU), Oman.

Mehdi Escrochi, Assistant Prof., of chemical and petroleum engineering department, Shiraz University, Shiraz, EOR Excellence Research Center.

Mohamad Vahid Afraz, holds B.Sc. degree of Chemical and Petroleum Engineering and he is research assistant in EOR Excellence Research Center, Shiraz University, Shiraz, Iran.

Golamreza Karimi, Associate Professor of Chemical Engineering, school of chemical and Petroleum Engineering, Shiraz University, Shiraz, Iran.

Yahya Al-Wahaibi, Associate Professor of Petroleum Engineering. Director of Oil and Gas Research Center, Sultan Qaboos University.

Shahab Ayatollahi, Professor, Director of EOR Research Center School of Petroleum and Chemical Engineering Shiraz University, Now with Sharif University of Technology.